



OPEN

Coral calcium carried hydrogen ameliorates the severity of non-alcoholic steatohepatitis induced by a choline deficient high carbohydrate fat-free diet in elderly rats

Kuai Ma¹, Xin Hu¹, Keiki Nambu², Daisuke Ueda³, Naotsugu Ichimaru⁴, Masayuki Fujino^{1,5}✉ & Xiao-Kang Li¹✉

Hydrogen has been reported to act as an antioxidant, anti-apoptosis and anti-inflammatory agent. Coral calcium carried hydrogen (G2-SUIISO) is a safer and more convenient form of hydrogen agent than others. The mechanism underlying the hepatoprotective effects of G2-SUIISO using an elderly non-alcoholic steatohepatitis (NASH) rat model was investigated. Two days after fasting, six-month-old elderly male F344/NSlc rats were given a choline deficient high carbohydrate fat-free (CDHCFF) diet from day 0 to day 3 as CDHCFF control group, and then switched to a normal diet from days 4 to 7 with or without 300 mg/kg G2-SUIISO. Rats in each group were finally being sacrificed on day 3 or day 7. In the CDHCFF diet group, G2-SUIISO decreased the liver weight-to-body weight ratio, the serum AST, ALT, total cholesterol levels, inflammatory infiltration, pro-inflammatory cytokine expression and lipid droplets with inhibiting lipogenic pathways by reducing sterol regulatory element-binding protein-1c, acetyl-CoA carboxylase and fatty acid synthase gene expression compared with the CDHCFF diet alone. G2-SUIISO had beneficial effects of anti-apoptosis as well the down-regulation of pro-apoptotic molecules including NF- κ B, caspase-3, caspase-9 and Bax. These findings suggest that G2-SUIISO treatment exerts a significant hepatoprotective effect against steatosis, inflammation and apoptosis in elderly NASH rats.

Abbreviations

ACC	Acetyl-CoA carboxylase
ALT	Alanine transaminase
AST	Aspartate transaminase
Bax	Bcl-2-associated X
CCR2	C-C chemokine receptor type 2
CDHCFF	Choline deficient high carbohydrate fat-free
FAS	Fatty acid synthase
FFAs	Free fatty acids
G2-SUIISO	Coral calcium carried hydrogen G2
HCC	Hepatocellular carcinoma
H ₂	Hydrogen
HSCs	Hepatic stellate cells

¹Division of Transplantation Immunology, National Research Institute for Child Health and Development, 2-10-1 Okura, Setagaya-ku, Tokyo 157-8535, Japan. ²Acche Corporation, Tokyo, Japan. ³Division of Hepato-Pancreato-Biliary Surgery and Transplantation, Department of Surgery, Kyoto University Graduate School of Medicine, Kyoto, Japan. ⁴Department of Urology, Kinki Central Hospital, Hyogo, Japan. ⁵Management Department of Biosafety, Laboratory Animal, and Pathogen Bank, National Institute of Infectious Diseases, 1-23-1, Toyama, Shinjuku-ku, Tokyo 162-8640, Japan. ✉email: mfujino-kkr@umin.ac.jp; ri-k@ncchd.go.jp

IL-6	Interleukin 6
IL-1 β	Interleukin-1 beta
IFN- γ	Interferon-gamma
iNOS	Inducible nitric oxide synthase
LDs	Lipid droplets
mRNA	Messenger RNA
NASH	Non-alcoholic steatohepatitis
NAFLD	Non-alcoholic fatty liver disease
NF κ B	Nuclear factor- κ B
OB-R	Leptin receptor
OPN	Osteopontin
ROS	Reactive oxygen species
RT-PCR	Real time-polymerase chain reaction
SREBP-1c	Sterol regulatory element-binding protein-1c
TC	Total cholesterol
TNF- α	Tumor necrosis factor-alpha

Non-alcoholic fatty liver disease (NAFLD) is the most common chronic liver disorder associated with metabolic dysfunction and is a leading cause of cirrhosis and hepatocellular carcinoma (HCC) with a global prevalence of 25%. It usually develops in the absence of excessive alcohol consumption and is associated with an unhealthy diet and lack of physical activity. Non-alcoholic steatohepatitis (NASH) is a progressive form of NAFLD, characterized by chronic inflammation and hepatocyte injury due to fat accumulation². A community-based study found that fatty liver is prevalent in the elderly population, with a prevalence of over 40%³.

Aging is a complex phenomenon characterized by the gradual decline of the tissue and organ function accompanying the irreversible age-related loss of viability. Impairment of the liver function and development of NAFLD are common among the elderly⁴. Accumulating evidence has pointed out that the process of aging itself markedly increases the prevalence of metabolic syndrome in humans, reportedly being a risk factor of NAFLD⁵, as it predisposes individuals to hepatic functional and structural impairment and metabolic risk. Oxidative stress is considered the primary cause of general aging as well as diseases associated with aging, especially metabolic diseases⁶. Oxidative stress, lipotoxicity and inflammation⁷ have been shown to play central roles in the development and progression of NAFLD. Furthermore, the progressively increased production of reactive oxygen species (ROS) during the aging process contributes to the accumulation of lipids, particularly cholesterol, in the liver of elderly individuals⁸.

Molecular hydrogen (H₂) was previously reported to act as an antioxidant for preventive and therapeutic applications by selectively alleviating cytotoxic oxygen radicals without affecting other ROS⁹. Previous studies have reported that H₂ functions as an antioxidant, anti-apoptosis and anti-inflammatory agent in many animal models and human clinical studies¹⁰. Among these studies, H₂ administration can be roughly divided into inhaling H₂ gas, drinking H₂ dissolved water and injecting H₂ dissolved saline¹¹. In our present study, we used coral calcium carried hydrogen (G2-SUIISO), which is a safer and more convenient form of H₂ agent than others, as the source of H₂. In general, H₂ cannot be kept in supplements as-is. Coral powder was therefore selected as the material to convey H₂, and we employed a unique method to successfully immobilize H₂ on the surface of the carrier coral calcium. When the coral calcium enters the body, hydrogen is generated upon contact with moisture.

The present study investigated the potential effects of G2-SUIISO with the goal of evaluating whether or not G2-SUIISO could attenuate the severity of NASH induced by a choline deficient high carbohydrate fat-free (CDHCFF) diet in elderly rats.

Results

G2-SUIISO attenuated CDHCFF-induced nonalcoholic steatohepatitis. As shown in Fig. 1B and Supplementary Fig. 3A, the liver weight-to-body weight ratio in the 3d_control group was significantly higher ($p < 0.0001$) than that in the Naïve group, while this value was lower ($p < 0.01$) in the 3d_G2 group. Furthermore, the liver weight-to-body weight ratio in the 7d_G2 group was down-regulated ($p < 0.05$) compared with the 7d_control group as well. The above results suggested that CDHCFF administration resulted in liver enlargement, and going back to eating normal diet again with G2-SUIISO treatment significantly attenuated this CDHCFF-induced liver enlargement.

NASH is characterized as the excessive accumulation of TC in lipid droplets (LDs) in hepatocytes, and ALT and AST activities are important biomarkers of liver damage or diseases⁸. G2-SUIISO significantly reduced the serum ALT, AST and TC levels in elderly NASH rats (Fig. 1C). The serum ALT and AST levels both notably differed between the 3d_control group and 3d_G2 group ($p < 0.001$), indicating that a CDHCFF diet caused severe hepatocellular injury in rats. Compared with the 3d_control group, the serum ALT and AST levels in the 3d_G2 group were markedly decreased. In addition, the serum TC levels were higher in the 3d/7d_control group than in the 3d/7d_G2 group ($p < 0.05$ and $p < 0.05$, respectively) suggesting that G2-SUIISO had notable effects of attenuating CDHCFF-induced NASH. In contrast, serum triglyceride (TG) was significantly decreased by CDHCFF diet and G2-SUIISO treatment showed comparable concentrations (Supplementary Fig. 3B). Based on the HE staining of liver specimens in Fig. 1D, we observed that the normal liver showed a clear and homogeneous texture, while the CDHCFF groups developed hepatocyte steatosis, ballooning and inflammatory cell infiltration on day 3 that was relieved on day 7. Compared with the CDHCFF diet groups, hepatocyte ballooning and steatosis in rat specimens were clearly reduced in the G2-SUIISO groups on days 3 and 7 (Fig. 1E, $p < 0.001$, $p < 0.001$, respectively), suggesting that G2-SUIISO ameliorated hepatic steatosis in NASH rats.

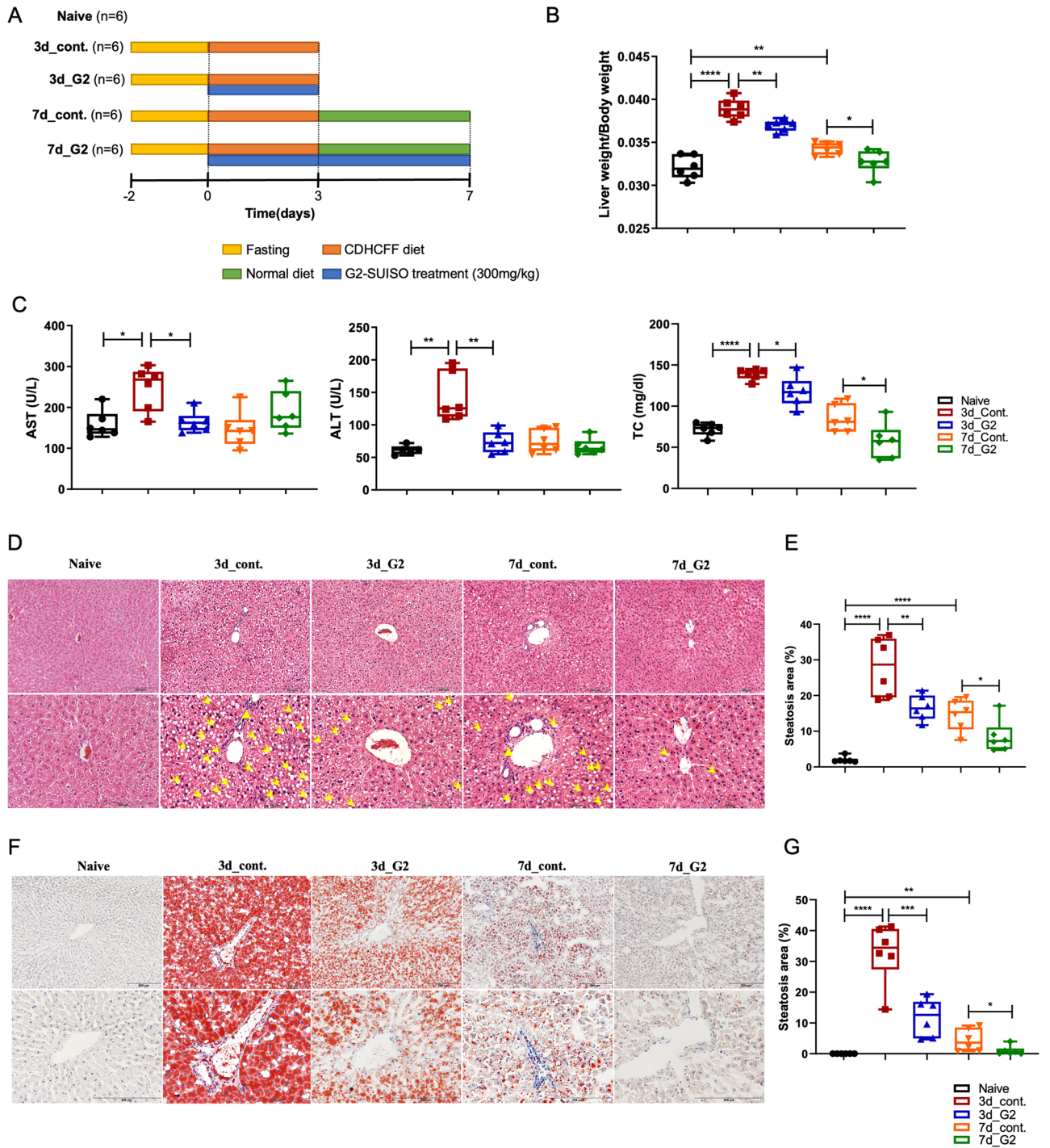


Figure 1. G2-SUISO attenuated CDHCF-induced nonalcoholic steatohepatitis. (A) The experimental design and timeline of the groups was shown. (B) The liver weight-to-body weight ratio in the five groups is shown. (C) G2-SUISO treatment significantly reduced serum ALT, AST and TC levels in NASH rats. (D) Hematoxylin and eosin (HE) staining of liver specimens in different groups suggested that G2-SUISO improved hepatic steatosis in NAFLD rats. The yellow triangle represents the area of inflammatory cell infiltration. White vacuoles showed lipids (yellow arrow) in HE staining (magnification $\times 100$ & $\times 200$). (E) An analysis of the HE staining of fatty liver specimens is shown. Each bar represents the mean \pm SD. (F) Liver sections of five groups were stained by Oil Red O solution. Red areas showed lipids in Oil Red O staining (magnification $\times 100$ & $\times 200$). (G) An analysis of the Oil Red O staining of fatty liver specimens is shown. Each bar represents the mean \pm SD; * $p < 0.05$, ** $p < 0.01$, *** $p < 0.001$, **** $p < 0.0001$.

To further explore the protective effects of G2-SUIISO on reducing steatosis in elderly NASH rats, liver sections from the five groups were subjected to Oil red O staining, which was used to measure fat loading in the hepatocytes. Based on Fig. 1E, we can see that G2-SUIISO decreased intracellular lipid deposition in the livers of the CDHCF group. A histological analysis of Oil Red O staining revealed a significant increase in intracellular lipid deposition in the livers of the 3d_CDHCF group and 7d_CDHCF group ($p < 0.0001$ and $p < 0.01$, respectively) (Fig. 1G). Numbers of LDs were markedly reduced in the livers of G2-SUIISO-treated mice on days 3 and 7 ($p < 0.001$ and $p < 0.05$, respectively).

G2-SUIISO exerted protective effects against inflammation. Among cytokine-related to the progression of NASH, tumor necrosis factor-alpha (TNF- α) plays a pivotal role in the inflammatory pathogenesis of NASH¹². As shown in Fig. 2A, hepatic mRNA expression of inflammatory cytokine-related genes, particularly TNF- α , inducible nitric oxide synthase (iNOS), osteopontin (OPN), interferon-gamma (IFN- γ), interleukin-1 beta (IL-1 β), IL-6 and C-C chemokine receptor type 2 (CCR2), were significantly higher following administration of an CDHCF diet. In contrast, the expression of TNF- α , iNOS and CCR2 was lower in the 3d_G2 group than in the 3d_control group ($p < 0.01$, $p < 0.05$ and $p < 0.01$, respectively). The IFN- γ , OPN, IL-1 β and IL-6 expression was down-regulated as well but without a significant difference. After the administration of G2-SUIISO for 7 days, TNF- α and IL-1 β showed notable reductions in expression ($p < 0.01$ and $p < 0.01$, respectively). The infiltration of neutrophils in liver was assessed using chloroacetate esterase staining of liver specimens. The hepatic expression of neutrophils was significantly increased in the CDHCF diet control group compared with Naive group on days 3 and 7 ($p < 0.05$ and $p < 0.05$, respectively) (Fig. 2B,C). Following the administration of G2-SUIISO, the neutrophil numbers in NASH liver specimens were reduced on days 3 and 7 ($p < 0.05$ and $p < 0.05$, respectively), and only a few scattered inflammatory foci were observed compared with

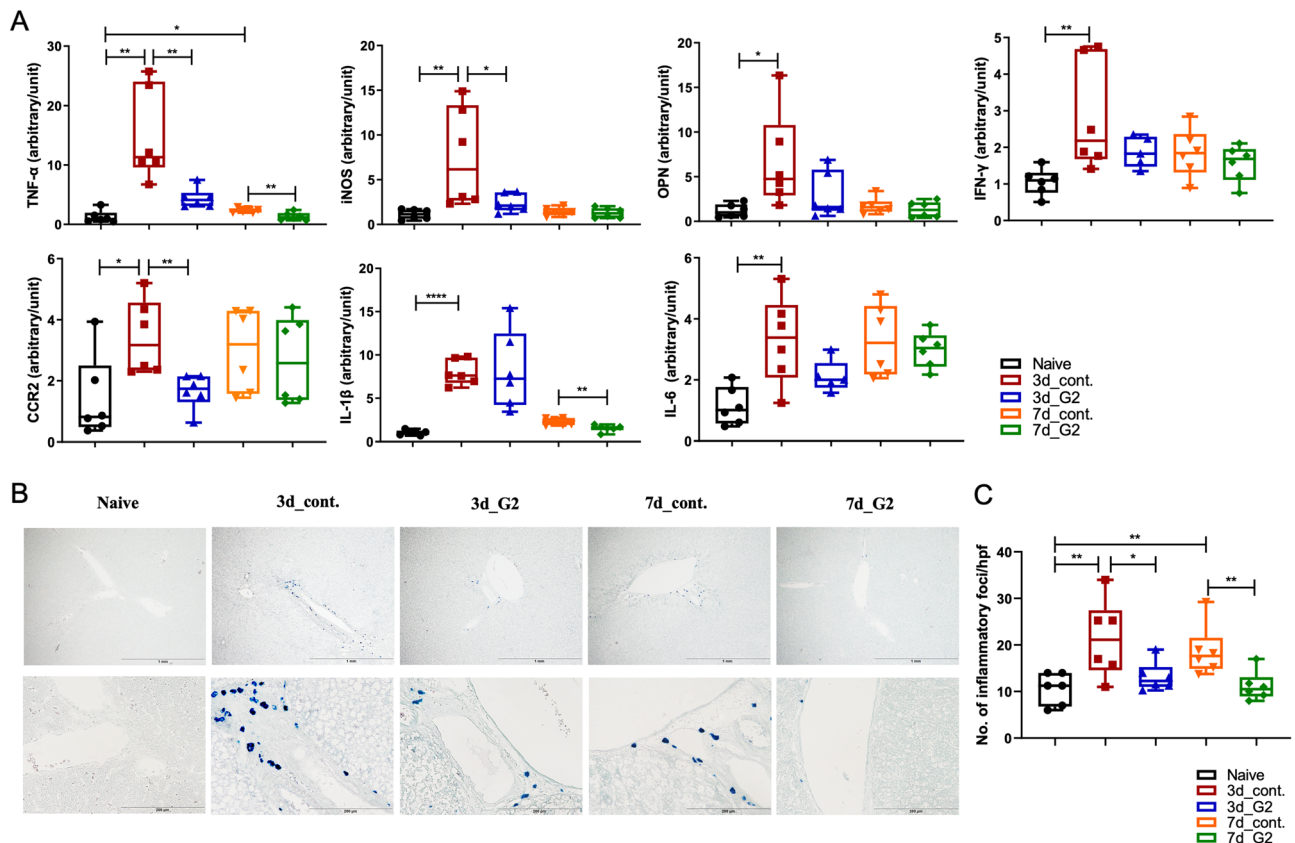


Figure 2. G2-SUIISO reduced the mRNA expression of inflammatory cytokine-related genes. (A) Homogenates of liver tissues were analyzed by qRT-PCR, as described in the Materials and Methods. The mRNA expression of inflammatory cytokine-related genes, particularly TNF- α , iNOS and CCR2, was significantly lower in the 3d_G2 group than in the 3d_control group. The mRNA expression of inflammatory cytokine-related genes, such as IFN- γ , OPN, IL-1 β and IL-6, tended to be down-regulated following G2-SUIISO treatment. Values are expressed as the mean \pm SD in arbitrary units; * $p < 0.05$, ** $p < 0.01$, **** $p < 0.0001$. (B) Chloroacetate esterase staining of liver specimens with inflammatory foci in the five groups is shown (magnification $\times 40$ & $\times 200$). (C) Analysis results of chloroacetate esterase staining of fatty liver specimens are shown. A total of 4 high power fields (hp/f) ($\times 40$) were randomly selected from each liver specimens ($n = 5$), and the number of inflammatory foci was counted. The data are expressed as the cell number/high-power field. Each bar represents the mean \pm SD; * $p < 0.05$.

the control group. In addition, the infiltration of T cells and macrophages in the liver was also analyzed using CD3 and ED1 monoclonal antibody. Both expressions in the liver specimens were increased in the 3d_CDHCFF group compared to the Naïve group ($p < 0.01$ and $p < 0.01$, respectively), and G2-SUISO treatment decreased the infiltration of CD3- and ED1-positive cells (Supplementary Fig. 2). Taken together, these findings suggested that G2-SUISO might prevent inflammation and inflammatory cell infiltration in the NASH elderly model liver.

G2-SUISO exerted anti-apoptotic effects. Previous studies have reported that increased hepatocyte apoptosis may play an important role in controlling the development of NASH¹³. As shown in Fig. 3A, the mRNA expression of apoptosis-related molecules, particularly Bax, caspase-1, caspase-3 and NF- κ B, was markedly up-regulated in the 3d_CDHCFF control group compared with Naïve group ($p < 0.0001$, $p < 0.001$, $p < 0.0001$ and $p < 0.0001$, respectively). The mRNA expression of Bax showed a significant decrease ($p < 0.05$) in the 7d_G2 group, and that of caspase-1, caspase-3 and NF- κ B showed decreasing trend. Furthermore, the mRNA expression of caspase-3 in the 3d_G2 group showed decreasing trend compared with the 3d_control group.

To confirm the anti-apoptosis effect of G2-SUISO, we measured the protein levels of caspase-1, caspase-3, caspase-9 and NF- κ B in liver tissues in the Naïve group, 3d_control group and 3d_G2 group by Western blotting (Fig. 3B). After a densitometric analysis of the signals, we found that the expression of caspase-3, caspase-9 and NF- κ B was significantly reduced by the treatment of G2-SUISO ($p < 0.05$, $p < 0.01$ and $p < 0.05$, respectively), whereas the caspase-1 expression showed no significant difference from before treatment.

G2-SUISO reduced steatosis in CDHCFF-induced NASH. As a pathological analysis showed that G2-SUISO reduced the lipid deposition caused by an CDHCFF diet in the liver (Fig. 1C–F), the mRNA expression of fatty acid uptake- and lipid metabolism-related cytokine-related genes in the five groups, particularly leptin receptor (OB-R), fatty acid synthase (FAS) and acetylCoA carboxylase (ACC), as well as sterol regulatory element-binding protein-1c (SREBP-1c) was measured. In Fig. 4, the mRNA expression of the OB-R, ACC and FAS genes increased significantly in the 3d_CDHCFF control group compared with the Naïve group ($p < 0.001$, $p < 0.0001$ and $p < 0.0001$, respectively). The SREBP-1c gene expression in the 3d_CDHCFF control group also showed an increasing trend but without significance. G2-SUISO markedly down-regulated the expression of OB-R compared with the 3d_CDHCFF control group ($p < 0.05$) and tended to down-regulate the expression of ACC and SERBP-1c. After 7 days of G2-SUISO administration, the mRNA expression of SREBP-1c, ACC

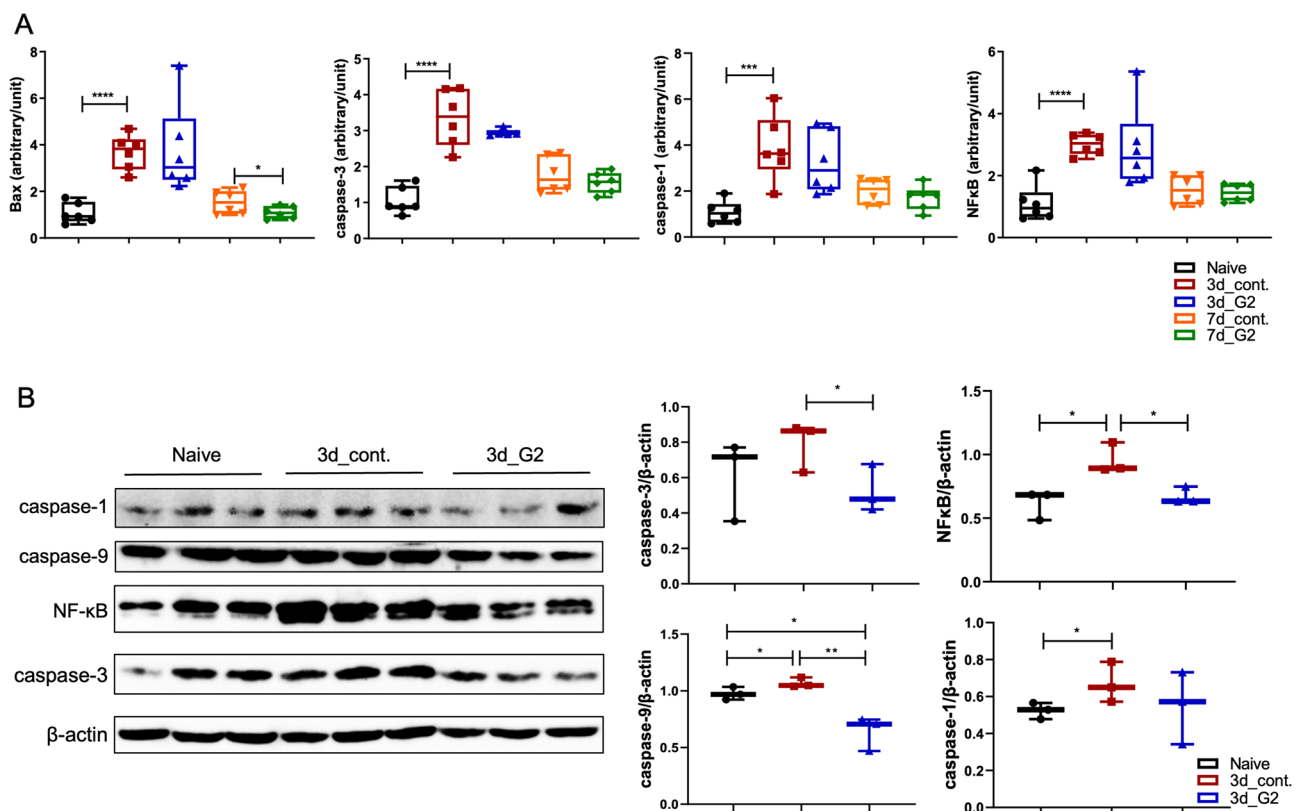


Figure 3. G2-SUISO reduced the mRNA expression of apoptotic molecules. (A) The mRNA expression of apoptosis-related genes in the five groups, particularly Bax, caspase-1, caspase-3 and NF- κ B, is shown. (B) Results of a Western blot analysis of caspase-1, caspase-3, caspase-9 and NF- κ B levels in the liver tissue of the Naïve group, 3d_control group and 3d_G2 group are shown. Data are expressed as the mean \pm SD; * $p < 0.05$, ** $p < 0.01$, *** $p < 0.001$, **** $p < 0.0001$.

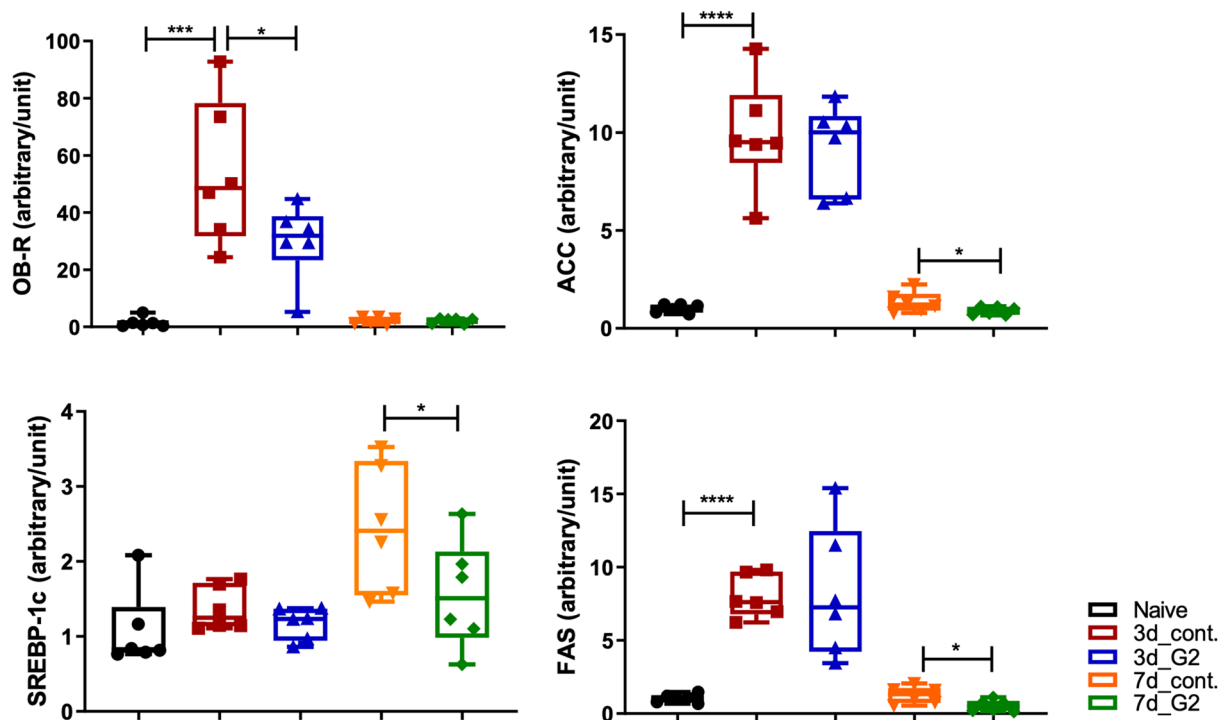


Figure 4. G2-SUIISO reduced hepatocyte steatosis in CDHCF diet-induced nonalcoholic steatohepatitis rat. The mRNA expression of fatty acid uptake- and lipid metabolism-related genes in the five groups, particularly leptin receptor (OB-R), fatty acid synthase (FAS) and acetylCoA carboxylase (ACC), as well as sterol regulatory element-binding protein-1c (SREBP-1c) are shown. Data are expressed as the mean \pm SD; * p < 0.05, ** p < 0.01, *** p < 0.001, **** p < 0.0001.

and FAS showed significant reductions (p < 0.05, p < 0.05 and p < 0.05, respectively). Furthermore, the mRNA expression of cholesterol metabolism genes, such as sterol regulatory element binding protein-2 (SREBP-2) or hydroxymethyl-glutaryl-CoA reductase (HMGCR) genes was increased by CDHCF diet and G2-SUIISO treatment showed the trend of decrease of the expression of these mRNA expression (Supplementary Fig. 3C).

Discussion

The prevalence of NAFLD has increased significantly in parallel with increasing rates of obesity, now being the most common cause of chronic liver disease worldwide¹⁴. NAFLD is reported to be a heterogeneous disease with a high prevalence in elderly patients, characterized by the accumulation of TG and fatty acids in hepatocytes¹⁵. Compared with younger groups, NAFLD in the elderly may carry a more substantial burden of hepatic and extrahepatic manifestations and complications¹⁶. Indeed, in our NASH model, aged rats showed more severe hepatitis when fed an CDHCF diet than young rats (Supplementary Fig. 1). H₂ has been reported to act as a therapeutic antioxidant by selectively reducing cytotoxic oxygen radicals, potentially leading to therapeutic effects in a variety of diseases, such as ischemia–reperfusion injury, colitis, NASH and aging-related diseases^{9,17–20}. G2-SUIISO is widely used in dietary supplement products (https://acche.co.jp/supplement/items_platinum/) as a safe and effective form of antioxidant with minimal side effects. This study demonstrated the promising potential effects of G2-SUIISO in a rat elderly model of NASH.

In this study, we used a CDHCF diet, which is one of the useful methods, to generate our NASH rat model^{21,22}. As expected, CDHCF diet-fed rats exhibited increased adipose tissue weights and liver weight-to-body weight ratios compared to the Naïve group (Fig. 1). In addition, the liver pathology summarized the major features of human NASH, including steatosis, ballooning degeneration and inflammation. With this model, the hepatic lipogenic/inflammation/apoptosis gene expression and serum biochemical markers, such as AST, ALT and TC, attenuation by G2-SUIISO showed convincing results for estimating the effect of the drug in our research. Oxidative stress and inflammation are the main components that contribute to the pathogenesis of NASH. It is widely acknowledged that TNF- α expression increases in cases of obesity and plays a major role in the inflammatory pathogenesis of NASH²³. Enrichment of innate immune cells and increased inflammation are hallmarks of NASH. Increasing evidence supports that neutrophils play a key role in the onset of NASH, and histological findings from human liver biopsies suggest that enhanced infiltration of neutrophils is one of the key histological features of NASH^{24,25}. Activation of the transcription factor NF- κ B also results in production of key chemokines for neutrophil recruitment²⁶. Steatosis is reported to lead to increased signaling of the transcription factor NF- κ B, which can induce the production of pro-inflammatory mediators, such as TNF- α , IL-6 and IL-1 β ²⁷. In addition, these pro-inflammatory cytokines contribute to the recruitment and activation of Kupffer cells to mediate inflammation in NASH. In our study, the mRNA expression of TNF- α significantly

decreased following the administration of G2-SUIISO to our rat NASH model (Fig. 2). The expression of other pro-inflammatory mediators, including IFN- γ , OPN, IL-1 β , CCR2, iNOS and IL-6, was markedly increased under CDHCF diet. Following G2-SUIISO treatment, most of these cytokines showed a down-regulated trend, suggesting that G2-SUIISO might have an anti-inflammatory effect. As shown in Fig. 3, down-regulation of NF- κ B by G2-SUIISO is one of the possible reasons for the reduction of pro-inflammatory molecules, while the mechanism of NF- κ B suppression by H₂ is still unclear²⁸. Other reasons may include induction of anti-inflammatory molecules. The trend toward enhanced mRNA expression of HO-1 was observed by G2-SUIISO administration (data not shown) and several studies demonstrated that HO-1 inhibits NF- κ B^{29–31}.

Previous studies have reported that cell death, including apoptosis, seems to play a vital role in the progression of NASH¹³. Apoptotic hepatocytes stimulate immune cells and hepatic stellate cells (HSCs) to progress to NASH and fibrosis through the production of inflammasomes and cytokines. NF- κ B is a master regulator of inflammation and cell death in the development of various liver diseases, such as NAFLD, hepatocellular injury, liver fibrosis and HCC³². The activation of NF- κ B in Kupffer cells or infiltrating monocytes is pro-inflammatory and induces the expression of death ligands, such as TNF- α ³³. Caspases are related to the induction of apoptosis, which is a mode of cell death regulated by homeostasis, supporting the coordinated demolition and clearance of aging and damaged cells³⁴. Bax belongs to the Bcl-2 protein family, and its pro-apoptotic function has been confirmed in many studies³⁵. The expression of these pro-apoptotic molecules was significantly up-regulated in the CDHCF diet control group on day 3 (Fig. 3). The administration of G2-SUIISO then down-regulated the pro-apoptotic molecules, such as NF- κ B and caspases, on day 3 according to our Western blot analyses. These findings suggest that G2-SUIISO may prevent apoptosis in the NASH model liver by inhibiting the expression of pro-apoptotic molecules.

In the present study, G2-SUIISO attenuated lipid accumulation in CDHCF-induced NASH in elderly rats. The reverse alterations in the hepatic lipid accumulation can be explained by the effects of G2-SUIISO on lipid metabolism. Previous studies have shown that the excessive hepatic accumulation of TG and FFAs induces hepatic steatosis^{36,37}. The present study demonstrated that treatment with G2-SUIISO ameliorated the lipid accumulation in the liver of CDHCF diet rats via the modulation of lipid metabolism-related molecules. The hepatic uptake of fatty acids is thought to occur via several mechanisms, including a transporter-mediated mechanism. In patients with NAFLD, the hepatic expression of fatty acid synthesis genes and fatty acid oxidation-related genes is up-regulated. ACC catalyzes the production of malonyl-CoA and is a major building block for de novo lipogenesis, promoting the oxidation of FFAs³⁸. SREBP-1c is a transcription factor that is a major regulator of FAS and other lipogenic proteins and is essential for the utilization and storage of glucose carbon³⁹. It regulates the onset of the lipogenic program and is able to bind to the promoters of several lipogenesis enzyme genes and induce their expression⁴⁰. The activity of the SREBP-1c/FAS pathway was previously shown to be markedly elevated and to contribute to the progression of hepatic steatosis in NASH mice⁴¹. Our present findings showed that G2-SUIISO significantly down-regulated SREBP-1c, FAS and ACC expression (Fig. 4), indicating that G2-SUIISO protects NASH rats from the SREBP-1c/FAS pathway. In this study, serum TG remained reduced after 2 days of fasting and feeding the CDHCF diet, with comparable concentrations with/without G2-SUIISO (Supplementary Fig. 3B). Previous study demonstrated that serum TG concentration was decreased after 2 days fasting but gradually increase after refeeding²¹. The reason why serum triglyceride levels are not increased by the CDHCF diet is still unclear, but one possible reason may be due to the use of rats of different species and ages in this study.

As shown in Fig. 5, hepatic FFAs in the liver were increased after feeding an CDHCF diet and accounted for the majority of the lipid accumulation, which can trigger NASH^{42,43}. Excessive consumption and dietary abnormalities (such as consuming an CDHCF diet after fasting) is related to oxidative stress in various tissues, including vessels, adipose tissues and the liver, and is consequent to disease development. Normally, oxidative stress, such as ROS, is continuously generated within cells but is counterbalanced by the antioxidant system to defend the body from cellular or tissue damage⁴⁴. In the progression of aging and lipogenesis, an imbalance of oxidant synthesis and antioxidants is the major contributor to the pathogenesis of NASH, leading to liver injury and hepatocyte deterioration⁴⁵.

Antioxidants have been suggested to be beneficial for health promotion and disease prevention. Chemiluminescence emission *in vitro* has been used to verify that H₂ can scavenge ROS markedly⁴⁶. Our results confirmed that the administration of G2-SUIISO, a proven safe and convenient antioxidant, improved NASH in our elderly rat model, probably due to its antioxidant activity. Hepatic and general serum marker levels including the liver weight-to-body weight ratio, AST and ALT were all improved, while FFA uptake-related, inflammatory and pro-apoptosis molecules were suppressed in the NASH liver by administration of G2-SUIISO. The beneficial effects of G2-SUIISO against hepatic steatosis in NASH elderly rats may be exerted through the inhibition of lipogenesis pathways by reducing SREBP-1c, ACC and FAS expression, thereby causing a reduction in the hepatic fat accumulation and a significant decrease in TC levels in serum. Overall, these results indicate that G2-SUIISO represents a simple and novel therapeutic strategy for NASH and NAFLD. Previous studies also showed that H₂ therapy is a very promising treatment of liver diseases and the rational use of it has already solved many problems clinically⁴⁷. However, the current clinical delivery method of H₂ is not very convenient, and G2-SUIISO can be made into capsules to solve this problem and facilitate H₂ administration.

Methods

Manufacturing method of G2-SUIISO. The original method of coral calcium carried hydrogen was described previously^{48,49}. The coral powder containing calcium carbonate was sealed into a pressure vessel, and gas with a concentration of 100% (vol) H₂ was circulated at a rate of 5 L/min at a temperature of 800 °C and pressure of 0.8 MPa, treated at a high temperature for 1 h. At 300 °C and 0.8 MPa, H₂ gas concentration of 100% (vol)

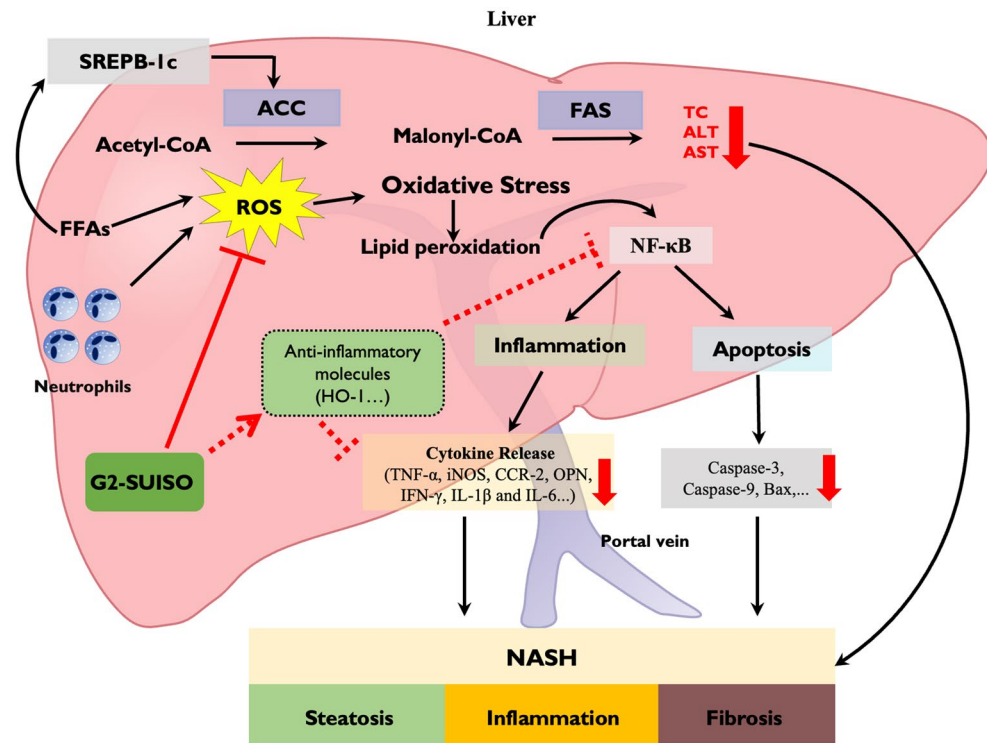


Figure 5. Schematic hypothesis of the mechanisms underlying the effects of G2-SUIISO for treating nonalcoholic steatohepatitis. The beneficial effect of G2-SUIISO against hepatic steatosis in NASH elderly rats may occur through the inhibition of lipogenesis pathways by reducing SREBP-1c, ACC and FAS gene expression, thereby causing a reduction in the hepatic fat accumulation and a significant decrease in total cholesterol (TC) levels in serum. The administration of G2-SUIISO can decrease lipid peroxidation and pro-inflammatory cytokines, such as TNF- α , iNOS, CCR-2, IFN- γ , OPN, IL-1 β and IL-6, which modulate liver damage in CDHCF diet-fed rats. G2-SUIISO might also up-regulated anti-inflammatory molecules, such as HO-1, which suppressed NF- κ B and inflammatory cytokine expression. G2-SUIISO is therefore able to reduce the activities of AST and ALT in the serum of NASH elderly rats. Furthermore, G2-SUIISO was found to exert anti-apoptotic effects as well by down-regulating pro-apoptotic molecules, such as caspase-9, caspase-3 and Bax via down-regulation of NF- κ B. Overall, this study provides evidence for the beneficial effects of G2-SUIISO in reversing the progression of NASH in elderly rats.

was circulated at a speed of 5 L/min and treated at a low temperature for 4 h. Finally, hydrogen powder with an average particle size of about 10 μ m was obtained by grinding.

Animal model. Six-month-old elderly male F344/NSlc rats (450–500 g) were purchased from Shizuoka Laboratory Animal Center (Shizuoka, Japan) and housed in a feeding room with automatically controlled light and temperature according to the guidelines of the Institutional Animal Care and Use Committee. All animal procedures were authorized by the National Research Institute for Child Health and Development (Permission No. A2020-004-C01-M01).

An acute NASH model was originally developed in 1997²¹ and is currently used in the field of fatty liver research with minor modification^{22,50–52}. As early as three days after starting the CDHCF diet, rats may develop hepatic inflammation. In our study, acute NASH in a rat model was induced by fasting for two days followed by feeding a CDHCF diet for three days. Rats in the present study were randomized into five groups as shown in Fig. 1A and as follows: (1) Naïve group (n = 6): rats received a normal diet and were gavaged with distilled water; (2) CDHCF control group on day 3 (3d_cont.) (n = 6): rats were fed an CDHCF diet from days 0 to 3 and then sacrificed on day 3; (3) CDHCF + G2-SUIISO-treated group on day 3 (3d_G2) (n = 6): rats had NASH induced, were gavaged with 300 mg/kg G2-SUIISO from days 0 to 3, and then were sacrificed on day 3; (4) CDHCF control group on day 7 (7d_cont.) (n = 6): rats were fed an CDHCF diet from days 0 to 3, switched to a normal diet from days 4 to 7, and then were sacrificed on day 7; (5) CDHCF + G2-SUIISO-treated group on day 7 (7d_G2) (n = 6): rats were fed an CDHCF diet from days 0 to 3 and then switched to a normal diet from days 4 to 7. At the same time, rats were gavaged with 300 mg/kg G2-SUIISO from days 0 to 7 before finally being sacrificed on day 7. At sacrifice, blood was collected, the liver weight-to-body weight ratio was measured, and the entire liver was removed for further analyses.

Serum biochemical analyses. Serum was collected from whole-blood samples after standing for 30 min at 37 °C and centrifuged at 3000 g for 20 min at 4 °C. The samples were then measured for the AST, ALT, TC and TG concentrations with a commercially available kit (Fujifilm, Tokyo, Japan) and an automatic biochemical analyzer (DRI-CHEM 3500i; Fujifilm) according to the manufacturer's instructions.

Histology and histopathological analyses. Liver tissues were cut and fixed in 10% formaldehyde solution for 48 h and embedded in paraffin for histological analysis. Sections of liver 4- μ m-thick were prepared and subjected to staining with hematoxylin and eosin (HE) (Muto Pure Chemicals, Tokyo, Japan) for morphological analyses to evaluate hepatocyte steatosis, ballooning and inflammatory cell infiltration. For another assessment of inflammatory cell infiltration, the quantification of neutrophils in liver specimens was stained using the Naphthol AS-D Chloroacetate Esterase Staining Kit (Muto Pure Chemicals). Slides were then examined by light microscopy (OLYMPUS, Tokyo, Japan) in a blind fashion to assess the inflammation state. Histological results were quantified using the WinRoof 7.4 software program (Mitani Corporation, Tokyo, Japan) as described previously⁵³.

Oil Red O staining. The frozen liver samples with optimal cutting temperature were cryo-sectioned at 5 μ m with a cryostat and then stained with Oil Red O working solution (Muto Pure Chemicals) for TG and FFA staining to evaluate hepatocyte steatosis⁵⁴. Results were quantified using the WinRoof 7.4 software program (Mitani Corporation) as well.

Immunohistochemical examinations. Immunohistochemical staining was performed on frozen sections using mouse anti-rat ED1 monoclonal antibody (Bio-Rad, Hercules, CA, USA) and Purified mouse anti-rat CD3 monoclonal antibody (BD Biosciences, San Diego, CA) as described previously⁵⁵.

Total mRNA preparation and quantitative reverse transcription polymerase chain reaction (qRT-PCR). Total mRNA was extracted from liver tissues using an RNeasy Mini Kit (Qiagen, Valencia, CA, USA). Each 0.8- μ g aliquot of mRNA was reverse-transcribed to cDNA using a Prime Script RT reagent Kit (RR037A; Takara, Shiga, Japan). qRT-PCR was performed by the SYBR[®] Green system using an Applied Biosystem PRISM7900 apparatus (Thermo Fisher Scientific, Waltham, MA, USA). The PCR cycle conditions for the SYBR[®] Green system were 50 °C for 2 min, 95 °C for 2 min, 45 cycles of 95 °C for 15 s and 60 °C for 60 s. The comparative cycle threshold (CT) method was used to determine the relative gene expression. The results of target genes (Table 1) were normalized by subtracting the CT value of 18S expression. The fold change was calculated by a comparative CT method as described previously⁵⁶.

Genes	Forward (5'-3')	Reverse (5'-3')	
SYBR green PCR system			
IFN- γ	GAAAGCCTAGAAAGTCTGAAGAAC	GCACCGACTCCTTTTCCGCTTCCT	
IL-6	TGATGGATGCTTCCAAACTG	GAGCATTGGAAGTTGGGGTA	
IL-1 β	CACCTTCTTTTCTTCATCTTTG	GTCGTTGCTTGTCTCTCCTTGTA	
CCR2	TTCTGGGCTCACTATGCTGC	AAGGGCCACAAGTATGCTGA	
Bax	CCAGGACGCATCCACCAAGAAGC	TGCCACACGGAAGAAGACCTCTCG	
Caspase-1	GTGTTGCAGATAATGAGGGC	AAGGTCCTGAGGGCAAAGAG	
Caspase-3	GGACCTGTGGACCTGAAAAA	GCATGCCATATCATCGTCAG	
Bcl-2	GGATGACTTCTCTCGTCGCTACCGT	ATCCCTGAAGAGTTCTCCACCAC	
NF κ B	GCATGCCATATCATCGTCAG	TGCTTCTCTCCCAGGAATA	
OB-R	TGCCTTGGAGGACTATGGGT	AGCCCCTTCAAAGACGAAG	
ACC	GCCTCTTCTGACAAACGAG	TCCATACGCCTGAAACATGA	
SREBP-1c	TGGATTGCACATTTGAAGACAT	GTCCTCTTTGATTCCAGGC	
FAS	CAGCTGTCAGTGTAAGAAACATGTC	AGCTCACGTGCAGTTAATTGTG	
HMGCR	CCCAGCCTACAACTGGAAA	CCATTGGCCTGGTACTCT	
SREBP-2	AGACTTGGTCATGGGGACAG	GGGGAGACATCAGAAGGACA	
18S	ATGAGTCCACTTTAAATCCTTTAACGA	CTTTAATATACGCTATTGGAGCTGGAA	
Genes	Forward (5'-3')	Reverse (5'-3')	Probe
Taqman probe PCR			
TNF- α	AATGGGCTCCCTCTCATCAGT	ACGGGCTTGTCACTCGAGTT	CCAGACCCTCACACTCAGATCATCTTCTCA
iNOS	GGACATTAACAACAACGTGGAGAA	AACCATTTTGTATGCTTGTGACTCTT	TGCTATTCAGCCCAACAACACAGG
OPN	CAAAGTCCAGGAGTTCCCTGTT	CTCTTCATGCGGGAGGTGA	TGATGAACAGTATCCCGATGCCACAGAT
18S	ATCCATTGGAGGGCAAGTCTGGTGC	ATGAGTCCACTTTAAATCCTTTAACGA	CTTTAATATACGCTATTGGAGGCTGGAA

Table 1. Primer sequences and probes used in this study.

Western blot analyses. Western blot analysis was performed as described previously²⁰. In brief, frozen liver tissues in the five groups were homogenized in RIPA buffer containing 1% protease inhibitor cocktail-1 and 1% protease inhibitor cocktail-2 (Sigma-Aldrich, St. Louis, MO, USA) followed by centrifugation in a microfuge at top speed for 30 min. Protein concentrations were assayed using a Bio-Rad Protein Assay (Bio-Rad). Samples were separated by electrophoresis on 10% polyacrylamide gels and transferred to Immobilon-PVDF (Bio-Rad). The membranes corresponding to the molecule of interest were cut out prior to hybridization with the antibody. After brief incubation with 5% non-fat milk to block non-specific binding, membranes were exposed overnight at 4 °C to specific caspase-1, caspase-3, caspase-9 and nuclear factor- κ B (NF- κ B). Protein expression was quantified by a laser densitometric analysis of the radiographic film using the ImageJ software program (NIH, Bethesda, MD, USA). The protein normalization was performed using β -actin as internal loading control.

Statistical analyses. The GraphPad Prism 9 software program (GraphPad, San Diego, CA, USA) was used to calculate statistical significance. Student's *t*-test was used for unpaired data. Data are expressed as the mean \pm standard deviation (SD). A value of $p < 0.05$ was considered to be statistically significant ($*p < 0.05$; $**p < 0.01$; $***p < 0.001$; $****p < 0.0001$).

Data availability

The datasets that support the findings of this study are available from the corresponding author on reasonable request.

Received: 27 March 2023; Accepted: 16 July 2023

Published online: 19 July 2023

References

- Powell, E. E., Wong, V. W. & Rinella, M. Non-alcoholic fatty liver disease. *Lancet* **397**, 2212–2224. [https://doi.org/10.1016/S0140-6736\(20\)32511-3](https://doi.org/10.1016/S0140-6736(20)32511-3) (2021).
- Fraille, J. M., Palliyil, S., Barelle, C., Porter, A. J. & Kovaleva, M. Non-alcoholic steatohepatitis (NASH)—a review of a crowded clinical landscape, driven by a complex disease. *Drug Des. Dev. Ther.* **15**, 3997–4009. <https://doi.org/10.2147/DDDT.S315724> (2021).
- Chen, T. P., Lai, M., Lin, W. Y., Huang, K. C. & Yang, K. C. Metabolic profiles and fibrosis of nonalcoholic fatty liver disease in the elderly: A community-based study. *J. Gastroenterol. Hepatol.* **35**, 1636–1643. <https://doi.org/10.1111/jgh.15073> (2020).
- Yang, J. *et al.* Oxidative stress and non-alcoholic fatty liver disease: Effects of omega-3 fatty acid supplementation. *Nutrients* <https://doi.org/10.3390/nu11040872> (2019).
- Sheedfar, F., Di Biase, S., Koonen, D. & Vinciguerra, M. Liver diseases and aging: Friends or foes? *Aging Cell* **12**, 950–954. <https://doi.org/10.1111/acel.12128> (2013).
- Finkel, T. & Holbrook, N. J. Oxidants, oxidative stress and the biology of ageing. *Nature* **408**, 239–247. <https://doi.org/10.1038/35041687> (2000).
- Chen, Z., Tian, R., She, Z., Cai, J. & Li, H. Role of oxidative stress in the pathogenesis of nonalcoholic fatty liver disease. *Free Radic. Biol. Med.* **152**, 116–141. <https://doi.org/10.1016/j.freeradbiomed.2020.02.025> (2020).
- Gao, Y. *et al.* Exercise and dietary intervention ameliorate high-fat diet-induced NAFLD and liver aging by inducing lipophagy. *Redox Biol.* **36**, 101635. <https://doi.org/10.1016/j.redox.2020.101635> (2020).
- Ohsawa, I. *et al.* Hydrogen acts as a therapeutic antioxidant by selectively reducing cytotoxic oxygen radicals. *Nat. Med.* **13**, 688–694. <https://doi.org/10.1038/nm1577> (2007).
- Hu, Q. *et al.* Molecular hydrogen: A potential radioprotective agent. *Biomed. Pharmacother.* **130**, 110589. <https://doi.org/10.1016/j.biopha.2020.110589> (2020).
- Iketani, M. & Ohsawa, I. Molecular hydrogen as a neuroprotective agent. *Curr. Neuropharmacol.* **15**, 324–331. <https://doi.org/10.2174/1570159x14666160607205417> (2017).
- Wigg, A. J. *et al.* The role of small intestinal bacterial overgrowth, intestinal permeability, endotoxaemia, and tumour necrosis factor alpha in the pathogenesis of non-alcoholic steatohepatitis. *Gut* **48**, 206–211. <https://doi.org/10.1136/gut.48.2.206> (2001).
- Kanda, T. *et al.* Apoptosis and non-alcoholic fatty liver diseases. *World J. Gastroenterol.* **24**, 2661–2672. <https://doi.org/10.3748/wjg.v24.i25.2661> (2018).
- Wang, X. J. & Malhi, H. Nonalcoholic fatty liver disease. *Ann. Intern. Med.* **169**, ITC65–ITC80. <https://doi.org/10.7326/AITC201811060> (2018).
- Noureddin, M. *et al.* Clinical and histological determinants of nonalcoholic steatohepatitis and advanced fibrosis in elderly patients. *Hepatology* **58**, 1644–1654. <https://doi.org/10.1002/hep.26465> (2013).
- Bertolotti, M. *et al.* Nonalcoholic fatty liver disease and aging: epidemiology to management. *World J. Gastroenterol.* **20**, 14185–14204. <https://doi.org/10.3748/wjg.v20.i39.14185> (2014).
- Nie, C. *et al.* Hydrogen gas inhalation alleviates myocardial ischemia-reperfusion injury by the inhibition of oxidative stress and NLRP3-mediated pyroptosis in rats. *Life Sci.* **272**, 119248. <https://doi.org/10.1016/j.lfs.2021.119248> (2021).
- Fu, Z., Zhang, J. & Zhang, Y. Role of molecular hydrogen in ageing and ageing-related diseases. *Oxid. Med. Cell Longev.* **2022**, 2249749. <https://doi.org/10.1155/2022/2249749> (2022).
- LeBaron, T. W. *et al.* Molecular hydrogen is comparable to sulfasalazine as a treatment for DSS-induced colitis in mice. *EXCLI J.* **20**, 1106–1117. <https://doi.org/10.17179/excli2021-3762> (2021).
- Li, S. W. *et al.* Hydrogen-rich water protects against liver injury in nonalcoholic steatohepatitis through HO-1 enhancement via IL-10 and Sirt 1 signaling. *Am. J. Physiol. Gastrointest. Liver Physiol.* **320**, G450–G463. <https://doi.org/10.1152/ajpgi.00158.2020> (2021).
- Delzenne, N. M., Hernaux, N. A. & Taper, H. S. A new model of acute liver steatosis induced in rats by fasting followed by refeeding a high carbohydrate-fat free diet. Biochemical and morphological analysis. *J. Hepatol.* **26**, 880–885. [https://doi.org/10.1016/S0168-8278\(97\)80256-5](https://doi.org/10.1016/S0168-8278(97)80256-5) (1997).
- Nagai, K. *et al.* Impact of venous-systemic oxygen persufflation with nitric oxide gas on steatotic grafts after partial orthotopic liver transplantation in rats. *Transplantation* **95**, 78–84. <https://doi.org/10.1097/TP.0b013e318277e2d1> (2013).
- Machado, M. V. & Diehl, A. M. Pathogenesis of nonalcoholic steatohepatitis. *Gastroenterology* **150**, 1769–1777. <https://doi.org/10.1053/j.gastro.2016.02.066> (2016).
- Cho, Y. & Szabo, G. Two faces of neutrophils in liver disease development and progression. *Hepatology* **74**, 503–512. <https://doi.org/10.1002/hep.31680> (2021).
- Wu, L. *et al.* The role of neutrophils in innate immunity-driven nonalcoholic steatohepatitis: Lessons learned and future promise. *Hepatol. Int.* **14**, 652–666. <https://doi.org/10.1007/s12072-020-10081-7> (2020).

26. Ishida, Y. *et al.* Opposite roles of neutrophils and macrophages in the pathogenesis of acetaminophen-induced acute liver injury. *Eur. J. Immunol.* **36**, 1028–1038. <https://doi.org/10.1002/eji.200535261> (2006).
27. Cobbina, E. & Akhlaghi, F. Non-alcoholic fatty liver disease (NAFLD)—pathogenesis, classification, and effect on drug metabolizing enzymes and transporters. *Drug Metab. Rev.* **49**, 197–211. <https://doi.org/10.1080/03602532.2017.1293683> (2017).
28. Russell, G., Nenov, A., Kisher, H. & Hancock, J. T. Molecular hydrogen as medicine: An assessment of administration methods. *Hydrogen* **2**, 444–460 (2021).
29. Yang, H. *et al.* Heme oxygenase-1 inhibits the proliferation of hepatic stellate cells by activating PPAR γ and suppressing NF- κ B. *Comput. Math. Methods Med.* **2022**, 8920861. <https://doi.org/10.1155/2022/8920861> (2022).
30. Bellezza, I. *et al.* Inhibition of NF- κ B nuclear translocation via HO-1 activation underlies α -tocopheryl succinate toxicity. *J. Nutr. Biochem.* **23**, 1583–1591. <https://doi.org/10.1016/j.jnutbio.2011.10.012> (2012).
31. Gao, W. *et al.* Dissecting the crosstalk between Nrf2 and NF- κ B response pathways in drug-induced toxicity. *Front. Cell Dev. Biol.* <https://doi.org/10.3389/fcell.2021.809952> (2022).
32. Luedde, T. & Schwabe, R. F. NF- κ B in the liver—linking injury, fibrosis and hepatocellular carcinoma. *Nat. Rev. Gastroenterol. Hepatol.* **8**, 108–118. <https://doi.org/10.1038/nrgastro.2010.213> (2011).
33. Ricchi, M. *et al.* Differential effect of oleic and palmitic acid on lipid accumulation and apoptosis in cultured hepatocytes. *J. Gastroenterol. Hepatol.* **24**, 830–840. <https://doi.org/10.1111/j.1440-1746.2008.05733.x> (2009).
34. Van Opdenbosch, N. & Lamkanfi, M. Caspases in cell death, inflammation, and disease. *Immunity* **50**, 1352–1364. <https://doi.org/10.1016/j.immuni.2019.05.020> (2019).
35. Guo, M. *et al.* Bax functions as coelomocyte apoptosis regulator in the sea cucumber *Apostichopus japonicus*. *Dev. Comp. Immunol.* **102**, 103490. <https://doi.org/10.1016/j.dci.2019.103490> (2020).
36. Choi, S. S. & Diehl, A. M. Hepatic triglyceride synthesis and nonalcoholic fatty liver disease. *Curr. Opin. Lipidol.* **19**, 295–300. <https://doi.org/10.1097/MOL.0b013e3282ff5e55> (2008).
37. Ong, K. T., Mashek, M. T., Bu, S. Y., Greenberg, A. S. & Mashek, D. G. Adipose triglyceride lipase is a major hepatic lipase that regulates triacylglycerol turnover and fatty acid signaling and partitioning. *Hepatology* **53**, 116–126. <https://doi.org/10.1002/hep.24006> (2011).
38. Fang, K. *et al.* Diosgenin ameliorates palmitic acid-induced lipid accumulation via AMPK/ACC/CPT-1A and SREBP-1c/FAS signaling pathways in LO2 cells. *BMC Complement Altern. Med.* **19**, 255. <https://doi.org/10.1186/s12906-019-2671-9> (2019).
39. Moon, Y. S. & Ali, S. Possible mechanisms for the equilibrium of ACC and role of ACC deaminase-producing bacteria. *Appl. Microbiol. Biotechnol.* **106**, 877–887. <https://doi.org/10.1007/s00253-022-11772-x> (2022).
40. Stoeckman, A. K. & Towle, H. C. The role of SREBP-1c in nutritional regulation of lipogenic enzyme gene expression. *J. Biol. Chem.* **277**, 27029–27035. <https://doi.org/10.1074/jbc.M202638200> (2002).
41. An, J. P. *et al.* Anti-hepatic steatosis activity of *Sicyos angulatus* extract in high-fat diet-fed mice and chemical profiling study using UHPLC-qTOF-MS/MS spectrometry. *Phytomedicine* **63**, 152999. <https://doi.org/10.1016/j.phymed.2019.152999> (2019).
42. Puri, P. *et al.* A lipidomic analysis of nonalcoholic fatty liver disease. *Hepatology* **46**, 1081–1090. <https://doi.org/10.1002/hep.21763> (2007).
43. Bechmann, L. P. *et al.* The interaction of hepatic lipid and glucose metabolism in liver diseases. *J. Hepatol.* **56**, 952–964. <https://doi.org/10.1016/j.jhep.2011.08.025> (2012).
44. Vona, R., Gambardella, L., Cittadini, C., Straface, E. & Pietraforte, D. Biomarkers of oxidative stress in metabolic syndrome and associated diseases. *Oxid. Med. Cell Longev.* **2019**, 8267234. <https://doi.org/10.1155/2019/8267234> (2019).
45. Oseini, A. M. & Sanyal, A. J. Therapies in non-alcoholic steatohepatitis (NASH). *Liver Int.* **37**(Suppl 1), 97–103. <https://doi.org/10.1111/liv.13302> (2017).
46. Deenin, W., Malakul, W., Boonsong, T., Phoungpetchara, I. & Tunsophon, S. Papaya improves non-alcoholic fatty liver disease in obese rats by attenuating oxidative stress, inflammation and lipogenic gene expression. *World J. Hepatol.* **13**, 315–327. <https://doi.org/10.4254/wjh.v13.i3.315> (2021).
47. Shi, J., Duncan, B. & Kuang, X. Hydrogen treatment: A novel option in liver diseases. *Clin. Med. (Lond.)* **21**, e223–e227. <https://doi.org/10.7861/clinmed.2020-0370> (2021).
48. Okuda, R. *et al.* Evaluation of released amount of hydrogen after high pressure hydrogen loading in carbonate. *Results Eng.* **4**, 100047. <https://doi.org/10.1016/j.rineng.2019.100047> (2019).
49. Li, H. *et al.* Hydrogen adsorption and desorption characteristics of heat-treated calcium carbonate derived from Akoya-Pearl-Oyster nacre. *J. Environ. Chem. Eng.* **8**, 103983. <https://doi.org/10.1016/j.jece.2020.103983> (2020).
50. Minor, T., Akbar, S., Tolba, R. & Dombrowski, F. Cold preservation of fatty liver grafts: prevention of functional and ultrastructural impairments by venous oxygen persufflation. *J. Hepatol.* **32**, 105–111. [https://doi.org/10.1016/s0168-8278\(00\)80196-8](https://doi.org/10.1016/s0168-8278(00)80196-8) (2000).
51. Miyachi, Y. *et al.* Etiology of liver steatosis influences the severity of ischemia/reperfusion injury and survival after liver transplantation in rats. *Liver Transpl.* **26**, 1504–1515. <https://doi.org/10.1002/lt.25814> (2020).
52. Okamura, Y. *et al.* Impact of subnormothermic machine perfusion preservation in severely steatotic rat livers: A detailed assessment in an isolated setting. *Am. J. Transpl.* **17**, 1204–1215. <https://doi.org/10.1111/ajt.14110> (2017).
53. Liu, C. *et al.* 5-ALA/SFC attenuated binge alcohol-induced gut leakiness and inflammatory liver disease in HIV transgenic rats. *Alcohol Clin. Exp. Res.* **43**, 1651–1661. <https://doi.org/10.1111/acer.14117> (2019).
54. Li, S. *et al.* Astaxanthin prevents ischemia-reperfusion injury of the steatotic liver in mice. *PLoS ONE* **12**, e0187810. <https://doi.org/10.1371/journal.pone.0187810> (2017).
55. Kawasaki, M. *et al.* Inducible liver injury in the transgenic rat by expressing liver-specific suicide gene. *Biochem. Biophys. Res. Commun.* **311**, 920–928. <https://doi.org/10.1016/j.bbrc.2003.10.085> (2003).
56. Zhao, J. *et al.* Monotherapy with anti-CD70 antibody causes long-term mouse cardiac allograft acceptance with induction of tolerogenic dendritic cells. *Front. Immunol.* **11**, 555996. <https://doi.org/10.3389/fimmu.2020.555996> (2020).

Acknowledgements

This study was supported by research grants from the Grant of Ministry of Education, Culture, Sports, Science and Technology of Japan (Grants-in-Aid 21K08634) and a Grant from the National Center for Child Health and Development (31-02).

Author contributions

X.K.L. conceptualized the study and all authors contributed to the study design. Data collection was conducted by K.M. The preparation of the research materials and data analysis were conducted by K.M., M.F., and X.K.L. Results and interpretations of the study data were discussed by all authors. The first draft of the manuscript was written by K.M., and all authors commented on earlier versions of the manuscript. All authors read and approved the final manuscript.

Competing interests

The authors declare no competing interests.

Additional information

Supplementary Information The online version contains supplementary material available at <https://doi.org/10.1038/s41598-023-38856-6>.

Correspondence and requests for materials should be addressed to M.F. or X.-K.L.

Reprints and permissions information is available at www.nature.com/reprints.

Publisher's note Springer Nature remains neutral with regard to jurisdictional claims in published maps and institutional affiliations.



Open Access This article is licensed under a Creative Commons Attribution 4.0 International License, which permits use, sharing, adaptation, distribution and reproduction in any medium or format, as long as you give appropriate credit to the original author(s) and the source, provide a link to the Creative Commons licence, and indicate if changes were made. The images or other third party material in this article are included in the article's Creative Commons licence, unless indicated otherwise in a credit line to the material. If material is not included in the article's Creative Commons licence and your intended use is not permitted by statutory regulation or exceeds the permitted use, you will need to obtain permission directly from the copyright holder. To view a copy of this licence, visit <http://creativecommons.org/licenses/by/4.0/>.

© The Author(s) 2023